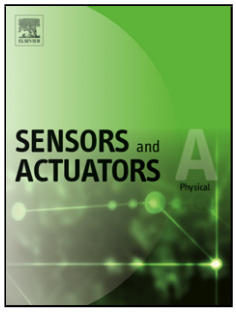

Title: Temperature dependence of a magnetically levitated electromagnetic vibration energy harvester

Authors: K. Pancharoen, D. Zhu, S.P. Beeby

PII: S0924-4247(17)30060-2
DOI: http://dx.doi.org/doi:10.1016/j.sna.2017.01.011
Reference: SNA 9967

To appear in: *Sensors and Actuators A*

Received date: 3-8-2016
Revised date: 5-12-2016
Accepted date: 9-1-2017

Please cite this article as: K.Pancharoen, D.Zhu, S.P.Beeby, Temperature dependence of a magnetically levitated electromagnetic vibration energy harvester, Sensors and Actuators: A Physical http://dx.doi.org/10.1016/j.sna.2017.01.011

Temperature dependence of a magnetically levitated electromagnetic vibration energy harvester

K Pancharoen[a], D Zhu[b], and S P Beeby[a *]

[a] *School of Electronics and Computer Science, University of Southampton, Southampton SO17 1BJ, UK*
[b] *College of Engineering, Mathematics and Physical Sciences, University of Exeter, Exeter, EX4 4QF, UK*

[*] Corresponding author. Tel.: +44 23 8059 6663
E-mail addresses: spb@ecs.soton.ac.uk

Highlights

- The performance of a magnetically levitated electromagnetic energy harvester under various ambient temperatures is investigated for the very first time.
- The structure of a magnet levitated harvester is proposed to study the temperatures effects on the fundamental properties of the harvester.
- Experiments are conducted to study parameters indicating the characterizations of the harvester, i.e. magnetic flux density, resonant frequency, damping ratio, quality factor, velocity of relative motion, and open circuit output voltage.
- Experimental and simulation results are presented and discussed.

Abstract

Electromagnetic vibration energy harvesters including magnetically levitated devices where opposing magnets are used to form the spring have been well documented. The strength of the magnets naturally has a large influence on the dynamic characteristics and output power of such harvesters. However, it can be affected by ambient temperatures which vary from applications to applications. This paper presents investigation into the performance of a magnetically levitated electromagnetic energy harvester under various ambient temperatures. Parameters investigated include magnetic flux density, resonant frequency, damping ratio, open circuit output voltage, velocity of the relative motion and the load resistance. Both simulation and experimental results show that these properties vary with ambient temperatures. The magnetic flux density reduces as the temperature increases which results in lower resonant frequency, lower relative velocity, lower open circuit output voltage and higher damping ratio. Varying resonant frequencies with temperature can lead to harvesters being de-tuned from the target vibration frequency. Decreasing magnetic field strength and increased damping ratios will also reduce output power even if the harvester's resonant frequency still matches the environmental vibration frequency. The power transferred to the electrical load will be reduced due to the variation in the optimal load resistance with temperature. This means the harvester is no longer matched to achieve the maximum harvested power. The specified maximum operating temperature of the magnets was found to lead to partial demagnetisation. When cycling from room to the maximum specified temperature, the magnetic field was initially found to fall but remained constant thereafter. Harvesters were found to operate beyond the specified maximum operating temperature of the magnet, but suffer from a reduced magnetic strength.

Keywords: Electromagnetic; Energy harvesting; Magnetic levitation; Magnetic spring; Temperature effect

1 Introduction

In recent years, energy harvesters have been widely developed for various applications due to their ability to generate power from the ambient environment and overcome the limitations of batteries such as finite lifetime, issue of disposal, limited power density, and cost of maintenance [1]. One of the most common energy harvesters is kinetic energy harvesters that convert energy in the form of vibrations or environmental motion into electrical energy typically using electromagnetic, piezoelectric or electrostatic transduction mechanisms.

Electromagnetic transduction has been achieved by exploiting relative movement between permanent magnets and a coil, by varying flux gradients intersecting a coil or a combination of these. The velocity of the relative movement between the magnets and coils, the number of coil turns, and the strength of the magnetic field all affect the amount of electrical energy that can be generated [2]. The temperature effects have been considered in some of the reported electromagnetic transducers especially in the processes of design and fabrication. Glynne-Jones et al [3] addressed the compatibility of working temperature and type of magnet to maintain strong flux density for a high degree of coupling. Neodymium-Iron-Boron (NdFeB) chosen for their electromagnetic generator in order to apply with the car engine which has a working temperature of up to 120°C. Zorlu et al [4] mentioned that the variation of the damping ratio with temperature has an influence on the analytical results of performance of the electromagnetic energy harvester proposed. The fabrication process of the electromagnetic energy harvester using buried NdFeB proposed by [5] was improved by maintaining process temperatures below 60°C in order to avoid the demagnetization of the magnetic film which otherwise would cause deterioration in the performance of the final device. These papers highlight the importance of considering temperature when fabricating or using electromagnetic transducers, but to the best of our knowledge the effects of temperature on electromagnetic vibration energy harvesters have not been discussed in details.

The temperature dependence of the coercive fields in permanent magnets has been investigated by Hu et al [6]. Magnets lose their magnetism when they are operated in an ambient temperature that exceeds their Curie temperature. It was also shown that the remanence and coercivity decrease with rising ambient temperature as characterised by the temperature-dependence equations presented by Calin et al [7]. Luo et al [8] highlighted that the effect of temperature should be considered alongside the grade of magnet used because the low Curie temperature of some magnets leads to a limited operating temperature range potentially close to room temperature that makes them unsuitable for many applications. Example specified temperature ranges for different types of applications include 0°C to 70°C for commercial, -20°C to 85°C for industrial, -40°C to 125°C for automotive and -55°C to 125°C for military. Typical temperature properties for a range of magnet materials are provided in Table 1.

Although the influence of temperature on magnetic properties has been widely investigated, characterization of electromagnetic energy harvesters under various ambient temperatures has not been well studied. The effects of temperature variations are an important consideration for all electromagnetic energy harvesters, and are especially relevant in the case of magnetically-levitated energy harvesters. Therefore, this paper studies the effects of temperature on the performance and fundamental properties of a magnetically-levitated energy harvester such as that shown in Fig. 1. The variation of magnetic flux density, the resonant frequency, damping ratio/quality factor, velocity of relative motion, open circuit output voltage and the optimal load resistance are all affected by temperature.

In this paper, the design and fabrication of the energy harvester used in the experiments is described. The theoretical background and the governing equations relating to magnetically levitated harvesters and magnetic characteristics are given in section 3. A comprehensive set of experimental and simulation results are presented and discussed in section 5.

2 Structure of the energy harvester

The harvester shown in Fig. 1 represents a standard configuration demonstrated in several devices in the literature [12–18], with some variations in the design and arrangement of the moving-mass components. Some of these harvesters were developed for harvesting energy from human movement which is characterized by low frequency high amplitude displacements [19,20]. The effect of temperature on the performance of such harvesters is least important in human applications due to the limited temperature range e.g. 0°C – 40°C. In contrast, this magnetically levitated configuration has also been applied for harvesting energy from tyre deformation. The harvesters were developed to power a wireless sensor network attached at the inner surface of the tyre for measuring the interaction between the road and vehicle, i.e. pressure, temperature and acceleration [16,21]. The standard automotive

temperature range is -40°C to 125°C and this is a real practical consideration since when traveling at a velocity of 100 km/h or when breaking from of 35 km/h tyre temperature can reach to 80°C and 90°C respectively [22,23].

The harvester studied in this work consists of two fixed magnets at the top and bottom of a Teflon tube. The tube contains a moving mass consisting of two magnets with a ferromagnetic spacer placed in between them in order to join the magnets together and concentrate the magnetic flux. In addition, the magnets have been aligned with like-poles facing each other as shown in Fig. 1. The magnetic flux density generated by the magnets at different temperatures was simulated by COMSOL as shown in Fig. 2. The voltage is induced in a stationary copper coil due to the variable and moving magnetic field that intersects it.

The interaction between the fixed and moving magnets results in nonlinear behaviour. The magnetic forces are nonlinearly varying with separation distance which results in a nonlinear magnetic spring. The properties of the magnetic spring are determined by the properties and strength of the magnets. Thermal demagnetization of the permanent magnets will reduce the performance of the harvester and change the dynamic behaviour of the magnetically levitated energy harvester. These effects will be explored using both simulations and experimental analysis and the results can be adapted for other types of devices.

3 Theoretical background

3.1 Magnet Characteristics

The magnet chosen for this work is NdFeB magnet (hard magnetic material) which has a high magnetic strength and magnetic coercivity [24–26]. The characteristics of a magnetic material are shown by its hysteresis plot, which illustrates the ability of a magnetic material to retain its magnetization. The hysteresis behaviour of each magnetic material is indicated by magnetic parameters such as coercivity (H_c) and remanence (B_r). The ability of the magnet to resist demagnetization is indicated by the value of coercivity (H_c) with higher values meaning it is more difficult to magnetise or demagnetise the material [27]. The residual magnetisation after the removal of the external magnetic force used to polarise the magnet is denoted by the remanence (B_r) [28]. The higher the remanence, the larger the magnetic flux density (B) produced by the magnet, for example, described by equation (1) which is an estimate of the magnetic flux density, B, produced by a cylindrical magnet [29].

$$( ) = \frac{}{2}\left(\frac{(+)}{\sqrt{(+)^2 + ^2}} - \frac{}{\sqrt{^2 + ^2}}\right) \tag{1}$$

where S is the distance from a pole face on the symmetrical axis (m), L is the length of magnet (m), and R is the radius of magnet (m). The relationship of remanence (B_r) and the coercivity (H_c) can be presented by [30]

$$\approx \quad _0 \tag{2}$$

Where $\mu_0 = 4\pi\times10^{-7}$ H/m is the permeability of free space and the coercive field $\mu_0 H_c$ is about 4-8% less than B_r. The information about the variation in these properties can be acquired by observing the demagnetization curves in the second quadrant of the hysteresis loop [31]. In this paper, the temperature coefficient of the remanence α_{B_r} has been used to estimate the change in remanence with temperature as expressed in % change per degree C by

$$= \frac{1}{}\cdot\frac{\Delta}{\Delta} \quad [\%/ \quad] \tag{3}$$

where T is temperature. The remanence at different temperatures can be estimated by multiplying the temperature coefficients with the temperature difference to obtain the percentage changes in expected B_r.

The Curie temperature, T_c, of NdFeB magnets varies depending upon the grade but typically ranges from 300 to 400°C, which is lower than some other rare-earth magnet such as Samarium-Cobalt (T_c 700 – 800°C) [32]. The practical maximum operating temperature will be less than the Curie temperature and hence the relatively low T_c limits their applications [33] [34]. In order to apply NdFeB magnets properly in particular applications, the temperature dependence of their magnetic properties should be appreciated.

3.2 Magnetically levitated Harvester

A conventional second-order spring, mass and damper system, as shown in Fig. 3, is typically used to model a linear inertial energy harvester. The magnetically-levitated harvester presented in this paper is further characterized using the nonlinear model due to nonlinear vibration of a magnetic spring. The governing equation can be derived by the equation of acting forces on the seismic mass, given by [35]

$$\ddot{(\ )} + \quad \dot{(\ )} + + \ (\ (\ )) + \quad = \quad - \quad \ddot{(\ )} \tag{4}$$

where $z(t)$ is the relative displacement of the seismic mass m and the base, c_m is the mechanical damping coefficient, θ is the electromagnetic coupling, is the electric current generated by the device, k and k_3 are linear and nonlinear spring stiffness respectively, $y(t)=Y\cos(\omega_d t)$ is the external excitation, the magnetic restoring forces F_S is characterised by the polynomial expansion of the relative displacement, $f(z)$. The Duffing equation is assumed to describe the nonlinear behaviour of the spring force. The first order and third order terms are considered as dominant terms, as shown in equation (5).

$$= \sum_{=0} \quad \approx \ _1 (\ ) + \ _3 \ ^3(\ ) \tag{5}$$

The term θi represents the electromotive force, which converts dissipated kinetic energy to electrical energy. This term can be transformed to a resistive force proportional to the relative velocity $z(t)$, as shown in equation (6).

$$\ddot{(\ )} + (\quad + \quad) \dot{(\ )} + \quad (\ ) + \ _3 \ ^3(\ ) = \quad - \quad \ddot{(\ )} \tag{6}$$

As a result, the damping coefficient, c, comprises of mechanical damping c_m and electrical damping c_e. From the above equation, the system characteristics can be analysed by the key parameters of conventional second-order spring, mass and damper system as follows.

$$= \sqrt{\ \ /\ \ } \ . \tag{7}$$

$$= \frac{\ \ }{2} = \frac{+}{2} \tag{8}$$

$$= 1/ \tag{9}$$

where ω_n is the natural frequency of the device, is the total damping ratio and Q is the Quality factor. These parameters are the key considerations for any further analysis (either analytical or numerical) of a magnetically levitated electromagnetic vibration energy harvester. The analysis of the energy harvester often involves determining the power transferred to the electrical load and the optimal load condition. Due to the complexity of nonlinear behaviours, the analysis can be achieved with the following simplifications [36,37]:

$$_{-} \quad = \quad + \frac{^2 \quad ^2}{(\ - \ ^2)^2 + (\quad)^2} \tag{10}$$

$$_{-} \quad = \frac{1}{8} \frac{(\quad)^2}{((\ - \ ^2)^2 + (\quad)^2) + \ (\quad)^2} = \frac{1}{8} \frac{^2 \ ^2}{\ \ } \left(1 - \frac{\ \ }{\ _{-}}\right) \tag{11}$$

where R_{L_opt} is the optimal load resistance, P_{L_opt} is the power transferred to an optimal load, R_C is the coil resistance, ω_d is the external exciting frequency and a is the excitation acceleration levels. However, in the levitated harvester, magnetic forces are acting in the place of a mechanical spring. Hence, the magnetic properties of the magnets will have a prominent effect on the characteristics of the harvester. In this paper, we show the effects of the ambient temperatures on the key parameters of the levitated harvester caused by the changes of mechanical and magnetic properties. The link between the key parameters and temperature is the magnetic force, and therefore the approximate model of the magnetic force (F_M) between two cylindrical magnets is given here for further reference [38].

$$= \frac{3(\quad {}_1^2{}_1)^2}{8}[\ (\ ) - \quad (\quad + \quad {}_2)], \text{where} \quad (\ ) = (\frac{1}{4} - \frac{{}_2^2+3\ {}^2}{3(\ {}_2^2+\ {}^2)^3}) \tag{12}$$

The equation of the magnetic force composes of the geometrical constants R_1, R_2, L_1 and L_2 of each cylindrical magnet where R represents the radius and L represents the length of the magnet (m). The function of F_M can be separated into two parts:

1) A constant term $= \frac{3(\quad {}_1^2{}_1)^2}{8}$
2) The function in terms of the relative distance between the two magnets, d.

The constant shows a second order relationship with magnetisation M ($\sim M^2$). This explicitly shows the connection between F_M and the temperature, since the magnetisation can be expressed by the terms of the temperature-related quantity B_r as $B_r = \mu_0 M$ [39]. Moreover, if B_r is assumed to vary linearly with temperature T in equation (3), F_M should vary quadratically with temperature. The second part of F_M is expressed by the function $f(d)$ in terms of the relative displacement between the associated magnets, therefore F_M can be transformed into a polynomial expansion

$$= \quad \sum_{=0}{}' \tag{13}$$

In the case of levitated devices, the magnetic forces are modelled as the nonlinear restoring spring force F_S, hence F_S is then represented by the total magnetic force of F_{M1} and F_{M2} as seen in Fig. 4.

Additionally, the relative displacements between magnets d_1 and d_1 can be expressed by an offset of the relative displacement z between the seismic mass and the base. So, F_S can be rewritten in a form of polynomial expansion in terms of z

$$= \quad {}_1 - \quad {}_2 = \quad \sum_{=0}{}^{\sim} \tag{14}$$

Assuming that the Duffing equation can closely explain the nonlinear behaviour of the device, F_S should be able to approximately fit into the polynomial form described in equation (5).

$$= \quad \sum_{=0}{}^{\sim} \quad \approx \quad {}_1^{\sim} + \quad {}_3^{\sim}\ {}^3 = \quad + \quad {}_3\ {}^3 \tag{15}$$

According to the equation (15), all stiffness coefficients of the nonlinear spring contain the constant term , derived from the magnetic force, therefore they can be rewritten in the quadratic form of the temperature. The experiment presented in section 5 will experimentally test this hypothesis for the relationship between the spring stiffness coefficients and temperature proposed in this section.

4 Experimental procedures

The Neodymium magnet used in this work is the sintered N35 grade NdFeB permanent magnets with a diameter of 4 mm and a thickness of 1 mm. Its magnetic properties are given in Table 2.

For the purposes of simulation, the values of remanence B_r at different temperatures obtained from the N35 magnet datasheet have been applied to the simulation model using COMSOL in order to calculate parameters, e.g., magnetic flux density, magnetic forces, and induced voltage. Although the value of remanence B_r provided in the datasheet was only stated at room temperature (20°C); the values at the temperature of 30°C, 40°C, 50°C, 60°C, 70°C, and 80°C can be calculated by using equation (3) and the temperature coefficient of remanence, α_{Br}, mentioned in Table 2. The values of remanence B_r at different temperatures are presented in Table 3. The simulation results from COMSOL will be compared with the experimental results in each section.

In order to study the temperature effect on the characteristics of the magnetically levitated harvester, the experiments have been separated into three sections. In section 5.1, static measurements of the magnetic flux density B of a N35 cylindrical magnet from room temperature to 80 °C are presented. This includes direct measurement of B on the top surface of the magnet using a Gauss meter model GMET H001. The variation of the quiescent position (z_0) and the magnetic forces (F_S) on the floating magnet at different temperatures are also presented. The quiescent position, z_0, was quantified in order to compare with the experimental results by calculating the position at which the magnetic forces, F_S, on the levitating magnet is equal the gravitational force, F_G, as given by

$$(\ _0) = \ _1(\ _0) - \ _2(\ _0) = \tag{16}$$

In this paper, the quiescent position (z_0) is one of the parameters used to indicate the strength of magnetic field under various ambient temperatures. Section 5.2 presents measurements of the dynamic properties of the harvester taken in an environment chamber. The electromagnetic energy harvester shown in Fig. 1 was tested on a shaker table located within the chamber in order to measure the resonant frequency and the output voltage of the harvester generated under various ambient temperatures. These measurements include stopping the shaker abruptly in order to record the attenuated impulse response of harvester, as shown in Fig. 5, which enables the harvester's damping factor to be calculated.

The damping factor can be determined from the system response using the following equation [41]:

$$= \frac{}{\sqrt{4 \ ^2 + \ ^2}} \tag{17}$$

where is the damping ratio, and α is defined as $= \frac{1}{} \ln \frac{1}{+1}$. The quality factor Q can be calculated from (9). This section also demonstrates how the velocity changes with temperature and discusses the variation in the voltage induced due to the change in velocity and magnetic flux density. The effect of the temperature on the value of the optimal load resistance is clarified in Section 5.2.4. Section 5.2.4 presents the influence of magnetic hysteresis on the performance of the levitated harvester. The ambient temperature of the harvester was cycled in an environmental chamber between temperature of 20°C and 80°C. This heating and cooling processes take 30 minutes per cycle. The change in the resonant frequency of the harvester after temperature cycling is recorded at 1 cycle, 5 cycles, 10 cycles, 15 cycles, 20 cycles, 30 cycles, 40 cycles, and 50 cycles.

5 Results and Discussion

5.1 Static characterization of magnets and harvester

The magnetic flux density B of the magnet was measured at various temperatures from 20°C to 80°C. Fig. 6 show the deterioration of magnetic flux density with rising temperature as measured by the experimentally and predicted by the COMSOL simulation results. There is a clear decrease in the magnetic flux density versus increasing temperature.

The effect of this decrease can be identified when observing the inertial mass position in the magnetically levitated harvester at different temperatures as shown in Fig. 7.

The initial moving-mass position decreases with increasing temperature. It can be described by the relation of magnetic flux density and magnetic force as expressed in equations (12). The reduced magnetic flux density of magnets due to the increased temperature reduces the magnitude of the force between moving mass and fixed bottom magnet which results in the reduced height of the quiescent position as illustrated in Fig. 7. Fig. 8 compares the

measured height and predicted height of the quiescent position calculated from the magnetic forces simulated by COMSOL using equation (16). The results from measurement and calculation are comparable and show a small offset of 0.3 mm approximately.

The offset is caused by the parameters used in the simulation, e.g, remanence B_r, which was an approximated value taken from the range of the values provided in the data sheet. Fig. 9 shows the simulation results of the total forces (F_S-F_G) on the levitated mass versus relative displacement, z, at different temperatures. The net force increases as the moving mass approaches the fixed top or fixed bottom magnets. Furthermore, it is clear that the net force decreases with the rising temperature.

5.2 Dynamic characterisation of the harvester

The fabricated harvester shown in Fig. 10 consists of two NdFeB cylindrical magnets pieces (Ø4 mm x 1 mm thickness) fixed in position at the top and bottom of the Teflon tube (Ø4.32 mm ID x 0.51 mm wall x 20 mm length). The coil is wound from Ø50 µm copper wire with 1,100 coil turns and this is positioned mid-way along the length of the tube. The moving mass was composed of two cylindrical Tungsten pieces (Ø4 mm x 1 mm thickness), two NdFeB magnets and a ferrite spacer with the same diameter of Ø4 mm as shown in Fig. 1. The harvester was tested on an electromagnetic shaker located inside an environmental chamber for temperature control. In order to measure the resonant frequency of the harvester, it was excited in the vertical direction at 500 m$\boldsymbol{g}$ (1$\boldsymbol{g}$ = 9.8m/s^2) in the temperature range of 20°C to 80°C. The measured resonant frequencies under various temperatures were compared with the simulation results predicted in COMSOL as presented in Fig. 11.

5.2.1 Resonant frequency and spring stiffness

To predict the resonant frequency of the harvester, the linear and nonlinear spring stiffness (k and k_3) at different temperatures are estimated by curve fitting on the net forces simulated in Fig. 9 (see Appendix A for details). The polynomial expansions of F_s from curve fitting can be aligned with the assumption of the nonlinear spring force described in equation (5). The spring stiffness parameters estimated from the fitting equations are presented in Table 4. Any variation in magnetic force results in the change of spring stiffness. For a fixed moving magnet displacement, a reduction in the magnetic forces will result in a lower spring stiffness, which lowers the resonance frequency of the energy harvester according to Eq. (7).

The polynomial fit has been applied on the stiffness-temperature curve to show the effect of temperature on the spring stiffness, k as shown in Fig. 12. This relation can be expressed in quadratic and cubic forms as

$$\text{Quadratic fitting:} \quad = -0.0007\ ^2 - 0.042\ + 6.9 \tag{18}$$

$$\text{Cubic fitting:} \quad = -6.9\ ^{-6}\ ^3 + 0.00034\ ^2 - 0.0054\ + 7.5 \tag{19}$$

According to the results from curve fitting, the quadratic form has given an acceptable approximation in comparison to the cubic form. The norms of residuals for quadratic and cubic fitting are 0.15423 and 0.11562 respectively. The dominant terms of both equations are the 1st order and the 2nd order. Therefore, this confirms the hypothesis that the function of spring stiffness, k. can be expressed in quadratic form as mentioned in section 3.2.

The resonant frequency reduces as the temperature is increased as shown in Fig. 11. This is due to the reduction in the magnetic forces as the consequence of the lower magnetic field as mentioned in Eq. (12) resulting in reduced spring stiffness as the relation in Eq. (15). This is a serious consideration for resonant energy harvesters tuned to a target frequency present in the environment. The change in resonant frequency could lead to a significant drop in the output of the harvester.

5.2.2 Mechanical damping factor

The mechanical damping factor was measured when the harvester is open circuit to minimise electrical damping. It was determined by monitoring the decay in the harvester output after stopping the driving vibrations. The damping ratio and quality factor Q can be calculated using equations (9) and (17). The dependence of damping ratio with temperature is shown in Fig. 13.

The damping ratio is linearly increasing with the rising temperature. This is due to the increasing friction between the moving mass and inner surface of the tube. This is due to the unequal thermal expansion coefficients of the materials

used in the harvester construction. The thermal expansion coefficient of Teflon tube (PTFE) is quite high; 143.3×10^{-6}/°C, when compared with other material as in Table 5 and this causes a reduction in the gap between the moving mass and the tube wall as the temperature increases.

This result is arguably more unforeseen than the previous results but is very important for the operation of the harvester. The level of damping reflects the level of unwanted mechanical losses and these losses increase at higher temperatures. The effect on the harvester of the increased losses is described as follows.

5.2.3 Open circuit voltage

Faraday's law describes the induced voltage. The electromotive force (*emf*) or voltage induced in a coil is proportional to time-rate change of magnetic flux linkage through a coil, given by [45]

$$= - — = - —— = - \dot{(\ )} = - \dot{(\ )} \tag{20}$$

where is induced voltage, is the total magnetic flux linking the coil, N is number of coil turns, B is the flux density, A is the area of the coil, l is length of a coil, and $z(t)$ is the velocity of the relative motion which can be determined from Eq. (6) as

$$\dot{(\ )} = \frac{\sqrt{1+(2\ —)^2}}{\sqrt{(1-(—)^2)^2+(2\ —)^2}} \sin(-) \tag{21}$$

where Y is the amplitude of external sinusoidal vibration, and is the phase angle. At resonance the induced voltage simplifies to

$$= - \frac{}{2} \tag{22}$$

Equation (22) succinctly summarises the effects of the change in magnetic and dynamic properties of the harvester on the output voltage. It is clear the magnetic flux density, B, has a direct effect on the induced voltage. The reduction in magnetic flux density due to the dependence of the remanence B_r (Eq. (1)) on temperature also reduces the spring constant, which in turn reduces the resonant frequency. The fall in the resonant frequency reduces the relative velocity of the magnets and this also reduces V_{emf}. The increase in the damping ratio with temperature will also reduce the velocity. The combined effect of the increasing damping ratio and decreasing resonant frequency on the relative velocity is shown in Fig. 14. The net effect on the induced voltage of these factors is shown in Fig. 15.

Fig. 15 shows the open circuit output voltage generated by the energy harvester when excited by an electromagnetic shaker under different temperatures. The excitation level was fixed at 500 m***g*** and the excitation frequency was varied to maintain resonance across the temperature range. The induced voltage is decreasing with rising temperature, which is consistent with the simulation result.

Since both B and velocity affect the induced voltage then, provided constant coil parameters, the decrease in B and velocity will both contribute to the lower induced voltage. Simplifying the harvester model as shown in Fig. 4 to describe the amount of voltage induced under the influence of B, it implies that the direct effect of the change in the magnetic flux density B is the most significant effect on the open circuit output voltage. Using the equations (5), (7) and rewriting the equation (22) (see Appendix B for details), the induced voltage is given by

$$= \frac{- \ ^2 \ ^2_1 \ _1}{_0} \sqrt{\frac{3\ [\ (\ )-\ (\ +\ _2)-\ (\ -\ -\ _1)-\ (\ -\ -\ _1+\ _2)]}{4}} \tag{23}$$

where D is the distance between fixed magnets, and function g is a function whose output value is dimensionless. It can be noted that the open circuit output voltage is proportional directly to the square of magnetic flux density.

5.2.4 Optimal load resistance

The effect of temperature on the values of the optimal load resistance R_{L_opt} at which the maximum power is obtained for a given frequency is presented in this section. The harvester was shaken at its resonant frequency and the value of the optimal load resistance was recorded for different ambient temperatures. The results are presented in Fig. 16. These results show good agreement with the results calculated using equation (10).

The results from Fig. 16 confirm that the relationship between the coil resistance R_C and the temperature can be expressed by a linear model as follows [46].

$$( ) = \_ [1 + (−)] \quad (24)$$

where R_{C_ref} is the coil resistance at reference temperature T_{ref}, usually 20°C, and $\alpha_C = 3.9\times10^{-3}$/°C is the temperature coefficient of resistance of copper. The values of coil resistance R_C increases with the temperature and can be further used to evaluate the optimal load resistance according to equation (10). At resonance, the expression in equation (10) can be simplified to

$$= + \frac{2}{} \quad (25)$$

The increasing value of R_C with the rising temperature affects the change in the values of R_{L_opt} as shown in Fig. 16. The values of R_{L_opt} increase with increasing temperature as well and come close to the values of R_C at high temperature (>70°C). It can be described by the relation presented in equation (25). As the temperature rises, the value of c_m increases while the values of θ decreases due to the reduction in magnetic flux density B, resulting in the convergence of R_{L_opt} to the value of R_C. As a result, the ratio between R_{L_opt} and R_C approaches unity and the power delivered to the load will be decrease with increasing temperature according to equation (11). This is shown in the results presented in Fig. 17.

5.3 Temperature cycle test

The influence of hysteresis behaviour of a magnet on the levitated harvester is investigated in this section by recording the resonant frequency of the harvester after every 5 cycles of temperature cycling between 20°C and 80°C. The results are presented in Fig. 18. After one cycle, the resonant frequency of the harvester decreases from 14.0 Hz to 12.0 Hz and then maintains in this level (about 12 Hz) for all subsequent cycles.

When the temperature of the harvester was cooled down back to room temperature, the original strength of magnets was not recovered because the maximum temperature in the cycle test reached the maximum operating temperature of the Neodymium magnets which is 80°C. However, the resonant frequency of the harvester does not degrade further because the temperature cycling is within the same range of temperature (20°C - 80°C).

6 Conclusion

This paper presents the influence of temperature on the performance of magnet levitated electromagnetic energy harvesters. Theoretical background about the harvester and magnetic properties has been provided with governing equation for further study. Six parameters indicating the characterizations of the harvester were investigated, i.e. magnetic flux density, resonant frequency, damping ratio, velocity of relative motion, open circuit output voltage, and optimal load resistance.

The analysis shows that the reduction of magnetic flux density with the rising temperature has an effect on performance of magnet levitated electromagnetic energy harvesters such as resonant frequency, open circuit voltage and potentially output power. These parameters start to decline significantly since 50°C which is 30 degree lower than the maximum operating temperature of the magnets used in the harvester. Variations in resonant frequency could mean the harvester is no longer tuned to the application. The increasing damping ratio with the increasing ambient temperature indicates higher parasitic damping from increased mechanical losses. The effect of temperature

on the value of the optimal load resistance can lead to a drop in the harvested power. These results highlight the importance of taking operating temperature into consideration when designing an electromagnetic energy harvester.

Whilst this analysis has focused on the magnetically levitated harvester architecture, other arrangements such as cantilever-based harvesters will be similarly affected. In the case of electromagnetic devices, the reduction in magnetic flux density will directly affect the harvester output. Changes to the stiffness of the cantilever material due to varying temperature (thermoelastic coefficient) should also be considered. The Young's modulus of cantilever materials will typically fall with increasing temperature causing a decrease in resonant frequency. Using more exotic materials such as Ni-Span-C that have a much lower thermoelastic coefficient typical metals can reduce this. This also potentially applies to piezoelectric harvesters but in this case the situation is more complicated due to the different thermal expansion coefficients of the cantilever and piezoelectric materials. Piezoelectric harvesters are also subject to the Curie temperature of the piezoelectric material but these tend to be higher than those of the rare earth magnets used here. Damping effects will depend on the mechanical design of the harvester and alternative architectures may not be affected by temperature.

Acknowledgement

This paper was performed under the SPHERE IRC funded by the UK Engineering and Physical Sciences Research Council (EPSRC), Grant EP/K031910/1. The authors would also like to acknowledge the support of Perpetuum Ltd. for the research facilities. All data supporting this study are openly available from the University of Southampton repository at http://dx.doi.org/10.5258/SOTON/381135

Appendix A

The polynomial fit has been applied on the magnetic restoring forces F_S as shown in Fig.18. The result of polynomial expansions is presented in Table 6.

Appendix B

The induced voltage in the equation (22) is rewritten in term of total force on the magnet $F_T = F_S - F_G$:

$$= - \quad \frac{}{2}\sqrt{\frac{2}{}} \tag{26}$$

Simplifying the equations (12) based on the simple diagram of force analysis in Fig. 4, the total force F_T is given by

$$= \frac{3(\quad {}_1^2 {}_1)^2}{8}[\ (\ ) - \ (\ + \ {}_2) - \ (\ - \ - \ {}_1) - \ (\ - \ - \ {}_1 + \ {}_2)] - \tag{27}$$

where R_1 is the radius of moving magnet, L_1 and L_2 are the length of moving magnet and fixed magnet respectively d is the distance between moving magnet and fixed magnet, D is the distance between fixed magnets, and F_G is the gravitational force which is small enough to be ignored. Substituting (27) into (26) produces the induced voltage in term of the magnetic flux density B in (23).

References

[1] S. Beeby, N. White, Energy Harvesting for Autonomous Systems, Artech House, Norwood, 2010.

[2] S. Beeby, N. White, Energy Harvesting for Autonomous Systems, Artech House, Norwood, 2010.

[3] P. Glynne-Jones, M.J. Tudor, S.P. Beeby, N.M. White, An electromagnetic, vibration-powered generator for intelligent sensor systems, Sensors Actuators, A Phys. 110 (2004) 344–349. doi:10.1016/j.sna.2003.09.045.

[4] Ö. Zorlu, E.T. Topal, H. Külah, A Vibration-Based Electromagnetic Energy Harvester Using Mechanical Frequency Up-Conversion Method, 11 (2011) 481–488.

[5] S. Miki, T. Fujita, T. Kotoge, Y.G. Jiang, M. Uehara, K. Kanda, K. Higuchi, K. Maenaka, Electromagnetic energy harvester by using buried NdFeB, Proc. IEEE Int. Conf. Micro Electro Mech. Syst. (2012) 1221–1224. doi:10.1109/MEMSYS.2012.6170409.

[6] J. Hu, X.C. Kou, H. Kronmüller, Investigation of the temperature dependence of the coercive fields in NdFeB magnets, Phys. Status Solidi. 138 (1993) K41–K44. doi:10.1002/pssa.2211380142.

[7] M.-D. Calin, E. Helerea, Temperature influence on magnetic characteristics of NdFeB permanent magnets, 2011 7Th Int. Symp. Adv. Top. Electr. Eng. (2011) 1–6.

[8] Y. Luo, N. Zhang, Temperature variation of domain structure and magnetization in NdFeB magnets, J. Appl. Phys. 61 (1987) 3445–3447. doi:10.1063/1.338748.

[9] Eclipse Magnetics, Magnetic Materials & Assemblies, (2014). http://www.eclipsemagnetics.com/row/magnet-materials-and-assemblies/ (accessed September 22, 2016).

[10] NdFeB Specialist E-Magnets UK, Temperature Ratings, (n.d.). http://www.ndfeb-info.com/temperature_ratings.aspx (accessed September 22, 2016).

[11] K. Pancharoen, D. Zhu, S.P. Beeby, A Hip Implant Energy Harvester, J. Phys. Conf. Ser. 557 (2014) 12038. doi:10.1088/1742-6596/557/1/012038.

[12] C.R. Saha, T. O'Donnell, N. Wang, P. McCloskey, Electromagnetic generator for harvesting energy from human motion, Sensors Actuators A Phys. 147 (2008) 248–253. doi:10.1016/j.sna.2008.03.008.

[13] A.R.M. Foisal, B.-C. Lee, G.-S. Chung, Fabrication and performance optimization of an AA size electromagnetic energy harvester using magnetic spring, 2011 IEEE SENSORS Proc. (2011) 1125–1128. doi:10.1109/ICSENS.2011.6126947.

[14] A.R.M. Foisal, G. Chung, Design and Analysis of a Vibration-driven AA Size Electromagnetic Energy Harvester Using Magnetic Spring, Trans. Electr. Electron. Mater. 13 (2012) 125–128. doi:10.4313/TEEM.2012.13.3.125.

[15] A. Munaz, B. Lee, G. Chung, Sensors and Actuators A : Physical A study of an electromagnetic energy harvester using multi-pole magnet, Sensors Actuators A. Phys. 201 (2013) 134–140. doi:10.1016/j.sna.2013.07.003.

[16] E. Bonisoli, A. Canova, F. Freschi, S. Moos, M. Repetto, S. Tornincasa, Dynamic simulation of an electromechanical energy scavenging device, IEEE Trans. Magn. 46 (2010) 2856–2859. doi:10.1109/TMAG.2010.2044156.

[17] Q. Zhang, Y. Wang, E.S. Kim, Power generation from human body motion through magnet and coil arrays with magnetic spring, J. Appl. Phys. 115 (2014). doi:10.1063/1.4865792.

[18] D.F. Berdy, D.J. Valentino, D. Peroulis, Kinetic energy harvesting from human walking and running using a magnetic levitation energy harvester, Sensors Actuators A Phys. 222 (2015) 262–271. doi:10.1016/j.sna.2014.12.006.

[19] T. Starner, J. a Paradiso, Human Generated Power for Mobile Electronics, Low-Power Electron. 1990 (2004) 1–30. doi:10.1.1.104.2324.

[20] T. Von Buren, P. Lukowicz, G. Troster, Kinetic energy powered computing - an experimental feasibility study, Seventh IEEE Int. Symp. Wearable Comput. 2003. Proceedings. (2003) 3–5. doi:10.1109/ISWC.2003.1241389.

[21] E. Bonisoli, F. Di Monaco, S. Tornincasa, F. Freschi, L. Giaccone, M. Repetto, Multi-physics optimisation of an energy harvester device for automotive application, COMPEL - Int. J. Comput. Math. Electr. Electron. Eng. 33 (2014) 846–855. doi:10.1108/COMPEL-10-2012-0208.

[22] W.Z.W. Zepeng, Finite Element Analysis of Mechanical and Temperature Field for a Rolling Tire, Meas. Technol. Mechatronics Autom. (ICMTMA), 2010 Int. Conf. 2 (2010) 278–283. doi:10.1109/ICMTMA.2010.42.

[23] Y. Malzahn, F. Kienhöfer, The effect of wheel configuration on vehicle component temperatures, in: HVTT13 Int. Symp. Heavy Veh. Transp. Technol. 13th, San Luis, Argentina, 2014.

[24] J. Fraden, Handbook of Modern Sensors: Physics, Designs, and Applications, 4th ed., Springer-Verlag New York, 2010. doi:10.1007/978-1-4419-6466-3.

[25] J.M.D. Coey, Rare-Earth Iron Permanent magnets, Oxford science publications, New York, 1996.

[26] T. Vaimann, A. Kallaste, A. Kilk, A. Belahcen, Magnetic properties of reduced Dy NdFeB permanent magnets and their usage in electrical machines, in: 2013 Africon, IEEE, 2013: pp. 1–5. doi:10.1109/AFRCON.2013.6757787.

[27] J. Karlsson, Review of Magnetic Materials Along With a Study of the Magnetic Stability and Solidity of Y40, (2012).

[28] A.R. Jha, Rare Earth Materials: Properties and Applications, CRC Press, 2014.

[29] J.M. Camacho, V. Sosa, Alternative method to calculate the magnetic field of permanent magnets with azimuthal symmetry, Rev. Mex. Fis. E. 59 (2013) 8–17.

[30] K. Halbach, Design of permanent multipole magnets with oriented rare earth cobalt material, Nucl. Instruments Methods. 169 (1980) 1–10. doi:10.1016/0029-554X(80)90094-4.

[31] S. Constantinides, D. Gulick, NdFeB for High Temperature Motor Applications, in: SMMA Fall Tech. Conf., 2004: pp. 1–33.

[32] J. Pyrhonen, T. Jokinen, V. Hrabovcova, Design of Rotating Electrical Machines, John Wiley & Sons, Ltd, West Sussex, 2008.

[33] S.R. Trout, Y. Zhilichev, Effective use of neodymium iron boron magnets, case studies, Proc. Electr. Insul. Conf. Electr. Manuf. Coil Wind. Conf. (Cat. No.99CH37035). (1999). doi:10.1109/EEIC.1999.826249.

[34] S.H. Kim, C. Doose, Temperature compensation of NdFeB permanent magnets, Proc. 1997 Part. Accel. Conf. (Cat. No.97CH36167). 3 (1997) 3227–3229. doi:10.1109/PAC.1997.753163.

[35] B.P. Mann, N.D. Sims, Energy harvesting from the nonlinear oscillations of magnetic levitation, J. Sound Vib. 319 (2009) 515–530. doi:10.1016/j.jsv.2008.06.011.

[36] M. Balato, L. Costanzo, M. Vitelli, Resonant electromagnetic vibration harvesters: Determination of the equivalent electric circuit

parameters and simplified closed-form analysis for the identification of the optimal diode bridge rectifier DC load, Int. J. Electr. Power Energy Syst. 84 (2017) 111–123. doi:10.1016/j.ijepes.2016.05.004.

[37] A. Cammarano, S.A. Neild, S.G. Burrow, D.J. Wagg, D.J. Inman, Optimum resistive loads for vibration-based electromagnetic energy harvesters with a stiffening nonlinearity, J. Intell. Mater. Syst. Struct. 25 (2014) 1757–1770. doi:10.1177/1045389X14523854.

[38] E. Varguez-Villanueva, V. Rodriguez-Zermeno, V. Sosa, Calculation of vertical force between finite, cylindrical magnets and superconductors, Rev. Mex. Física. 54 (2008) 293–298.

[39] B.A.D. Piombo, A. Vigliani, E. Bonisoli, Dynamics of suspensions with rare-earth permanent magnets, in: G.S. Agnes, K.-W. Wang (Eds.), Smart Struct. Mater. 2003 Damping Isol., 2003: pp. 106–115. doi:10.1117/12.483817.

[40] Magnet Expert Ltd., Grades Of Neodymium Magnets, (n.d.). http://www.first4magnets.com/tech-centre-i61/information-and-articles-i70/neodymium-magnet-information-i82 (accessed April 20, 2015).

[41] W.T. Thomson, Theory of vibration with application, 4th ed., Nelson Thornes Ltd, 2003.

[42] S. Stoupin, Y. V. Shvyd'Ko, Thermal expansion, Phys. Rev. Lett. 104 (2010). doi:10.1103/PhysRevLett.104.085901.

[43] A. Technologies, Material Expansion Coefficients, Laser Opt. User's Man. (2002) 17-1-12.

[44] Bal Seal Engineering, Coefficient of Thermal Expansion for Various Materials, 18 (2004) 1–6.

[45] M. Mizuno, D.G. Chetwynd, Investigation of a resonance microgenerator, J. Micromechanics Microengineering. 13 (2003) 209–216. doi:10.1088/0960-1317/13/2/307.

[46] J.H. Dellinger, The temperature coefficient of resistance of copper, Govt. Print. Off., 1911.

Biographies

K. Pancharoen received the B.Sc. degree in electrical engineering from Thammasat University (Thailand), and the M.Sc. degree in Microelectromechanical Systems (MEMS) from University of Southampton. She is currently a full time PhD student in Electronics and Electrical Engineering research group (EEE) of the School of Electronic and Computer Science (ECS) at the University of Southampton under supervision of Professor Steve Beeby and Dr.Dibin Zhu. Her research focuses on the energy-harvesting device, hip implant harvesting within the SPHERE project, for powering autonomous body-worn healthcare devices.

D. Zhu received BEng in Information and Control Engineering from Shanghai Jiao Tong University, China, in 2004 before joining University of Southampton in October 2004. He was awarded MSc in RF Communication Systems in 2005 and PhD in Electrical and Electronic Engineering in 2009, respectively. He is currently a Lecturer in Energy Harvesting Research Group, College of Engineering, Mathematics and Physical Sciences, University of Exeter, UK. His research interests include energy harvesting from various sources (vibration, wind, human movement, etc.), self-powered systems and wireless power transfer. He has over 60 publications in these fields.

S.P. Beeby obtained his BEng (Hons) in mechanical engineering in 1992 and was awarded his PhD in 1998. He was appointed a Reader in 2008 and was awarded a personal Chair in 2011. His research interests include energy harvesting, e-textiles, MEMS, active printed materials development and biometrics. He leads the UK's Energy Harvesting Network and is Chair of the International Steering Committee for the PowerMEMS conference series. He is currently leading 3 UK funded research projects and has previously been principal or co-investigator on a further 18 projects and co-ordinated 2 European Union research projects. He has co-authored/edited three books including 'Energy Harvesting for Autonomous Systems' (Artec House, Inc., Boston, London, 2010). He has given 14 invited talks and has over 200 publications and 10 patents. He has an H-Index of 39 with >9000 citations. He is a co-founder of Perpetuum Ltd., a University spin-out based upon vibration energy harvesting formed in 2004, Smart Fabric Inks Ltd., and D4 Technology Ltd

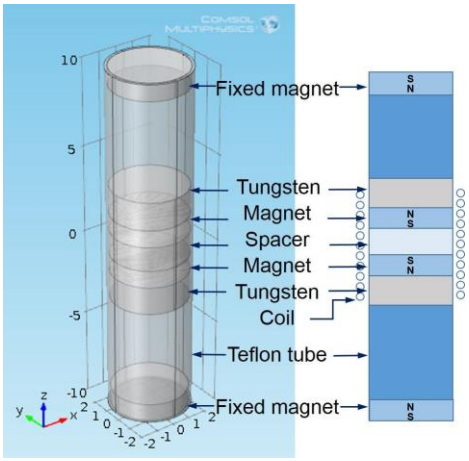

Fig. 1. Schematic of magnet levitated harvester [11].

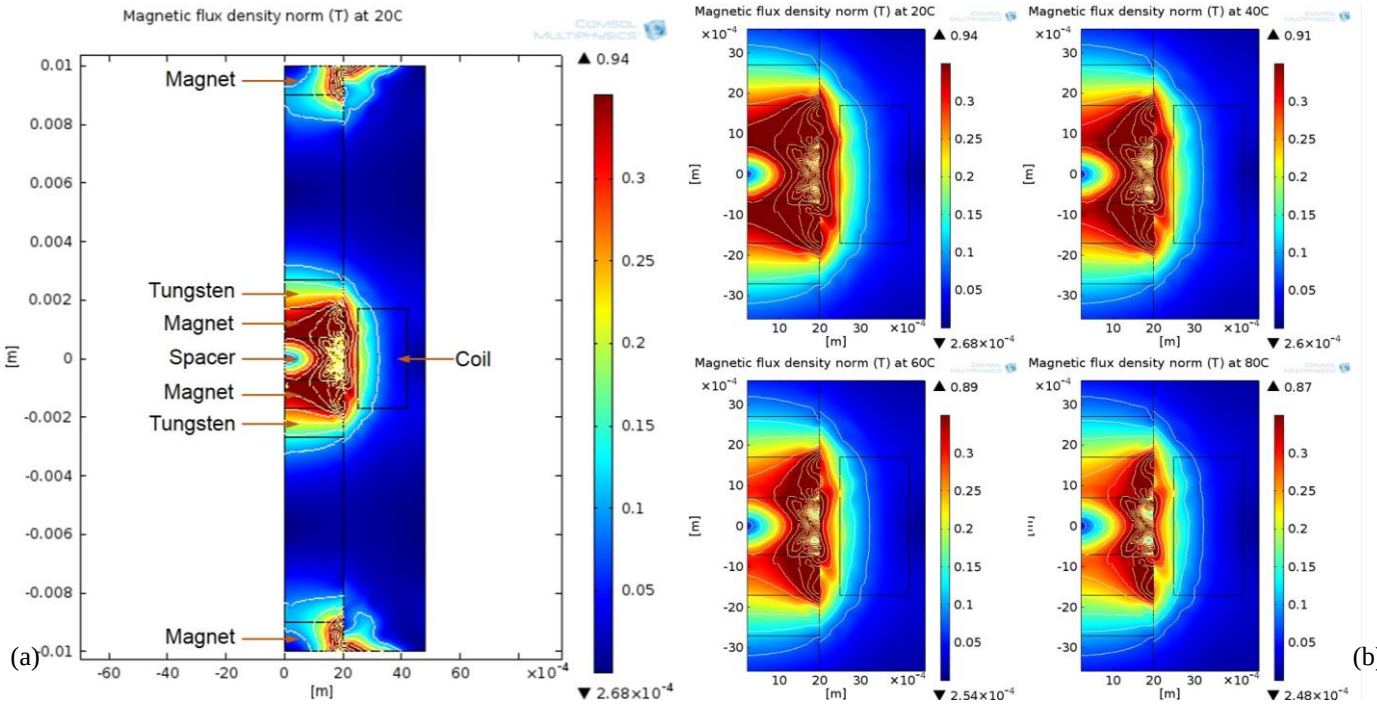

Fig. 2. (a) The magnetic flux density of the harvester with (b) zoomed view around the moving magnet and a stationary copper coil at temperature of 20°C,40°C, 60°C, and 80°C.

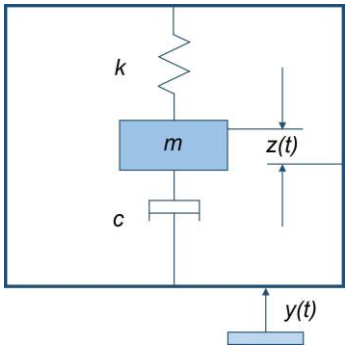

Fig. 3. Model of second-order spring-mass system.

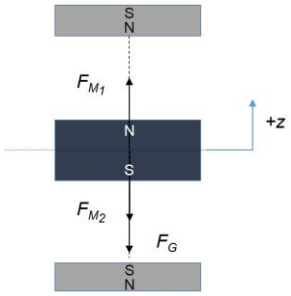

Fig. 4. Diagram of force analysis on the moving magnet.

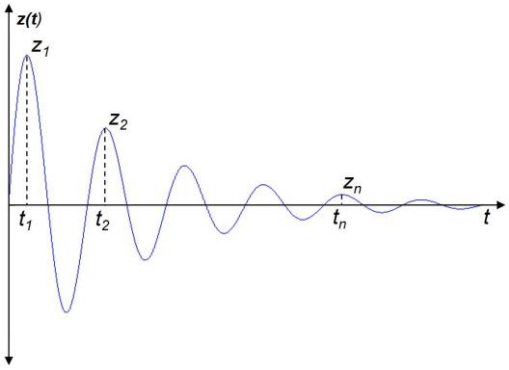

Fig. 5. Example of an underdamped impulse response [41].

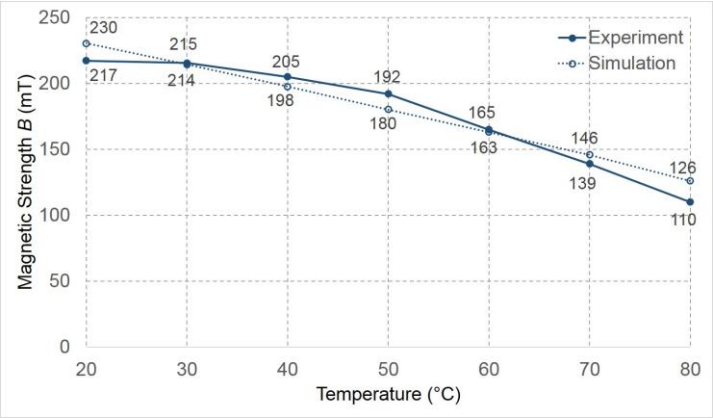

Fig. 6. Dependence of N35 NdFeB magnetic flux density on temperature.

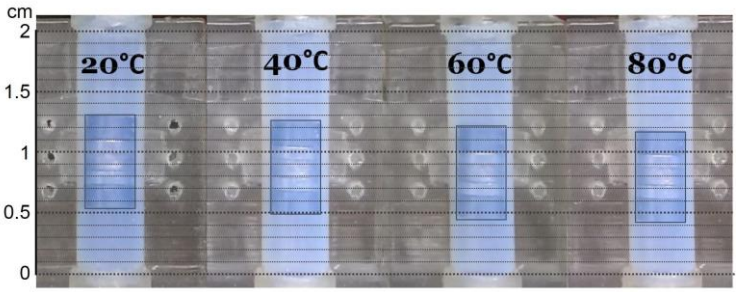

Fig. 7. The quiescent position of moving mass at different temperature.

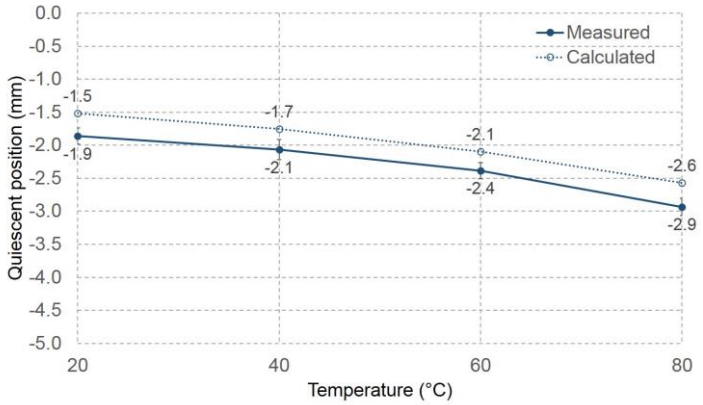

Fig. 8. Measured and calculated quiescent position of the levitating mass at different temperature.

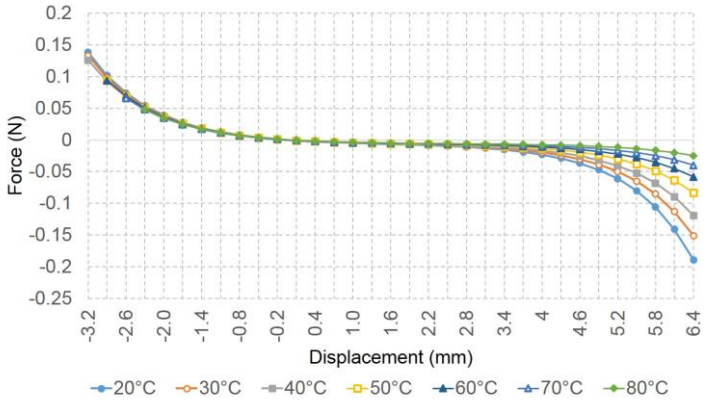

Fig. 9. Trend of total forces on moving magnet at different temperatures.

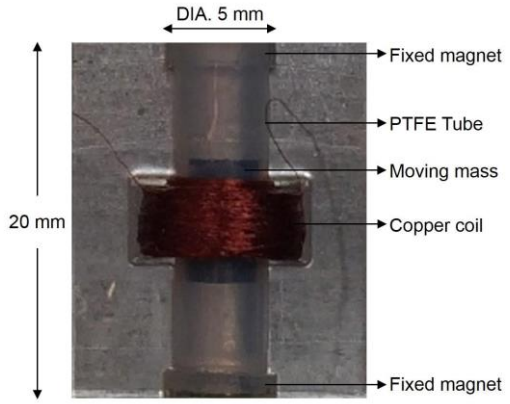

Fig. 10. Fabricated electromagnetic-based harvester.

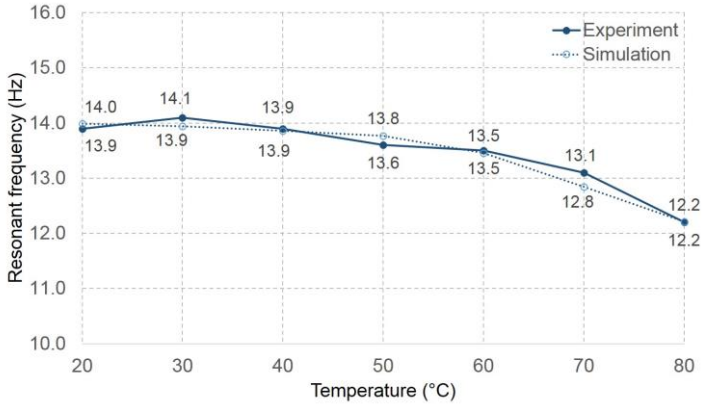

Fig. 11. Variation of resonant frequency with temperature.

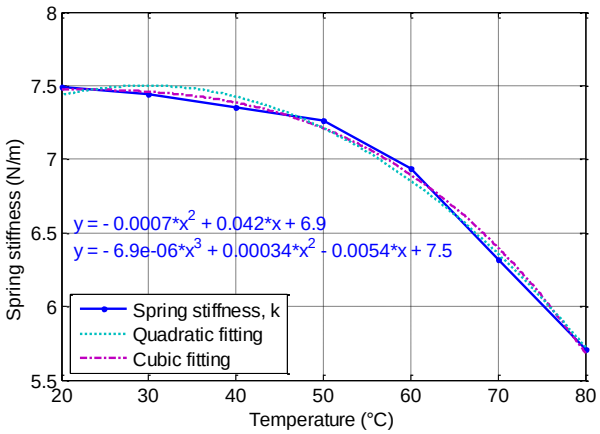

Fig. 12. The spring stiffness estimated from curve fitting at different temperatures.

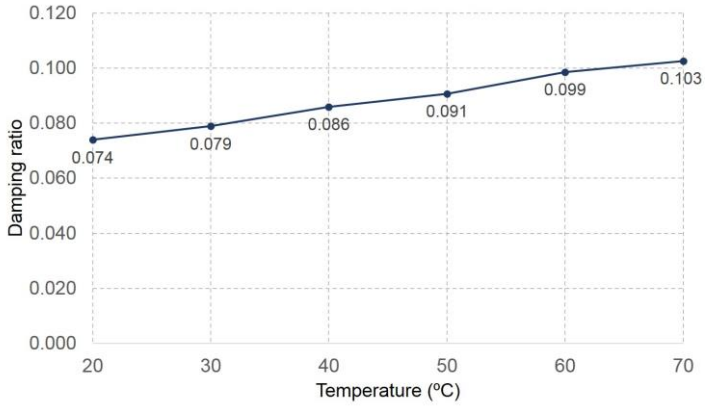

Fig. 13. Variation of damping ratio with temperature.

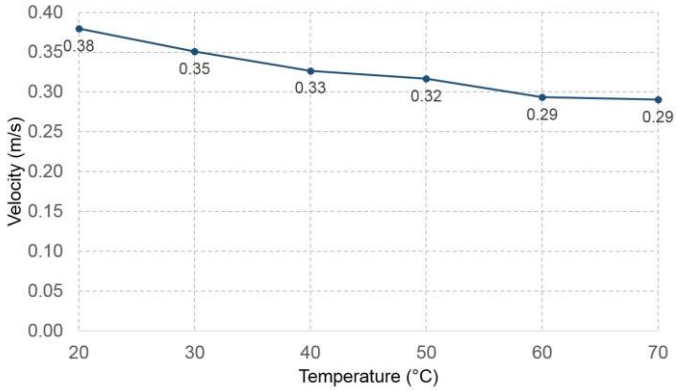

Fig. 14. Variation of velocity with temperature.

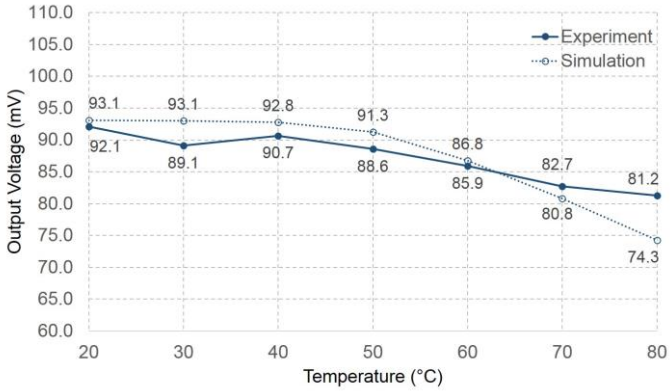

Fig. 15. Output voltage generated under various temperatures.

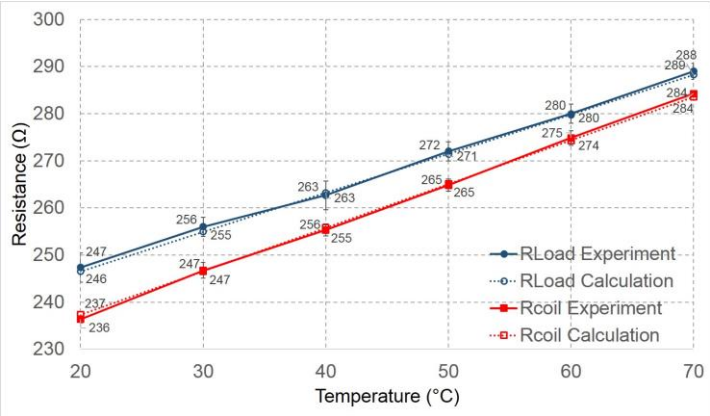

Fig. 16. Variation of optimal load and coil resistances with temperature.

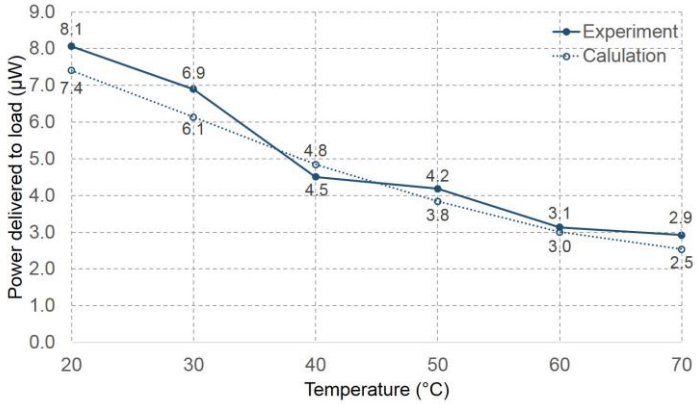

Fig. 17. Variation of power transferred to load with temperature.

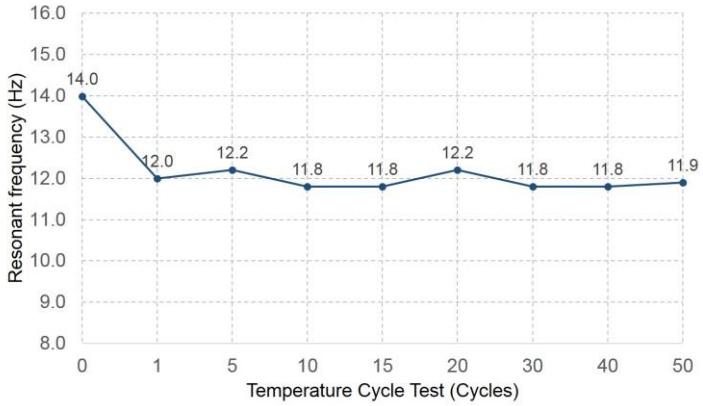

Fig. 18. Variation of damping ratio with temperature.

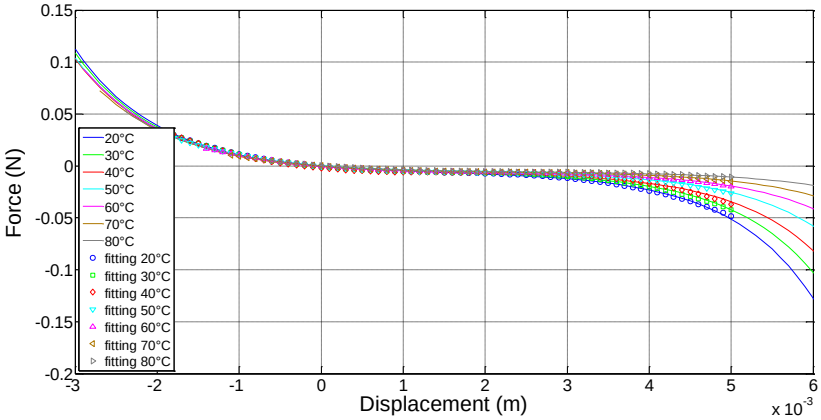

Fig. 19. The spring stiffness estimated from curve fitting at different temperatures.

Table 1
Typical Temperature properties of magnet materials [9,10].

Properties	Neodymium magnets	Samarium Cobalt Magnets	Alnico Magnets	Ferrite Magnets
Max. Operating Temperature	80°C	300°C	450°C	250°C
Min. Operating Temperature	-138°C	-273°C	-75°C	-20°C
Curie Temperature	310°C	700°C	800°C	450°C
Temp. coefficients of Induction, α_{Br}	-0.12%/°C	-0.05%/°C	-0.03%/°C	-0.2%/°C
Temp. coefficients of Coercivity, α_{Hci}	-0.6%/°C	-0.3%/°C	-0.02%/°C	+0.27%/°C

Table 2
Magnetic properties of N35 NdFeB magnets at room temperature [32,40].

Properties	Parameter	Value	Unit
NdFeB magnet grade	-	N35	-
Remanence	B_r	1170-1220	mT
Coercive Force	H_c	≥ 868	kA/m
Intrinsic Coercive Force	H_{ci}	≥ 955	kA/m
Max. energy product	$(BH)_{max}$	263-287	kJ/m^3
Max. Operating Temperature	-	80	°C
Temp. coefficient of remanence		-0.12	%/°C
Temp. coefficient of coercivity		-0.6	%/°C

Table 3
The remanence of N35 NdFeB magnets at different temperatures.

Temperature (°C)	20	30	40	50	60	70	80
Remanence, B_r (Tesla)	1.20	1.18	1.17	1.15	1.14	1.13	1.11

Table 4
The spring stiffness of the harvester at different temperatures.

Temperature (°C)	20	30	40	50	60	70	80
Linear spring stiffness, k (N/m)	7.49	7.44	7.35	7.26	6.94	6.32	5.71
Nonlinear spring stiffness, k_3 (N/m)	8.34e-5	8.14e-5	8.46e-5	5.89e-5	4.55e-5	3.48e-5	2.48e-5

Table 5
The coefficient of thermal expansion of materials used in harvester fabrication [42–44].

Material	Value	Unit
NdFeB	3.4	10^{-6}/°C
Tungsten	4.9	10^{-6}/°C
Mild steel	13	10^{-6}/°C
PTFE	143.3	10^{-6}/°C

Table 6
The polynomial expansions of force-displacement curves.

Temperature	3	2	1	0
20°C	-833844.0283	3755.451266	-7.494303267	-0.000592863
30°C	-813634.8015	3906.201334	-7.441319928	-0.00092614
40°C	-845979.7011	4302.427261	-7.354845779	-0.00193796
50°C	-588988.3477	3359.023612	-7.262607462	-0.000437754
60°C	-454591.6369	2865.933576	-6.939243244	4.80197E-05
70°C	-347932.2447	2402.409255	-6.318461113	0.000118443
80°C	-247647.9073	1932.077884	-5.707279781	0.0002867